RSC Advances

PAPER

View Article Online
View Journal | View Issue

Cite this: *RSC Adv.*, 2024, **14**, 32852

Effect of catalyst and oxidant concentrations in a TEMPO oxidation system on the production of cellulose nanofibers†

Jisoo Park,[a] Danbee Lee,[ab] Kyojung Hwang,[a] Jimin Lee,[a] Tai-Ju Lee,[c] Youngsu Kim,[a] Jung Hyeun Kim,[d] Jieun Lee,[a] Won-Jae Youe,[a] Sang-Jin Chun*[a] and Jaegyoung Gwon*[a]

In traditional TEMPO oxidation systems, the high cost of TEMPO catalysts has been a significant barrier to the industrialization of oxidized CNF. From an economic perspective, presenting the characteristics of various CNFs produced with the oxidation systems with reduced catalyst usage could facilitate the industrial application of CNF across a wide range of fields. In this study, it was demonstrated that reducing the amount of TEMPO catalyst used (from 0.1 to 0.05 mmol g^{-1}) in a conventional oxidation system increased the carboxylate content by approximately 6.3%. Furthermore, the activation of hydroxyl amine TEMPO, which is generated after the oxidation reaction of cellulose, was enhanced by adjusting the dosage of the inexpensive oxidant NaClO, leading to a 20% improvement in carboxylate content. This suggests that controlling the amount of NaClO as an oxidant can be a key parameter in adjusting the dosage of TEMPO to achieve the targeted degree of surface substitution. Results from the dispersion stability, UV-transmittance, and morphological properties of TEMPO-oxidized CNF using microfluidizing treatment showed that high carboxylate content plays a crucial role in producing high-purity CNF suspensions, which are small, uniform, and free from microfibers. Additionally, by varying the number of mechanical treatments applied to the oxidized cellulose, various types of CNF suspensions with different mean widths were obtained. We expect that these findings offer meaningful insights to end-users seeking a breakthrough in the performance limitations of final applications using cellulose nanomaterials.

Received 9th July 2024
Accepted 28th September 2024

DOI: 10.1039/d4ra04948a

rsc.li/rsc-advances

Introduction

Using polymers derived from natural sources continues to be a pressing challenge in modern society, with growing global awareness of environmental problems linked to plastic pollution. Cellulose nanomaterials (CNMs) possess significant potential as green materials owing to their unique structure, remarkable mechanical performance, biodegradability, sustainability, and abundance.[1] CNMs—the most abundant nano-sized fibers in nature—are mainly obtained from plant cell walls and consist of fibrils with widths of 2–20 nm that enhance their mechanical properties.[2] Cellulose nanofibers (CNFs) are a type of CNM prepared by extracting individual cellulose fibrils from natural cellulose through mechanical fibrillation. They typically have a diameter of 15–30 nm and a length on the scale of microns.[3,4] Natural materials such as bleached wood pulp and cotton linters can be used for producing CNFs, which can have high crystallinity in the range of 65–95%, depending on the characteristics of the raw material.[5–7] CNFs exhibit unique properties such as low density, large specific surface area, and high strength owing to their nanoscale size.[8] Moreover, they improve the performance of materials integrated with them in high-tech fields.[9–12] Therefore, CNF applications are continuously being explored across various fields of material science.

However, CNF manufacturing solely *via* mechanical fibrillation is difficult because individual cellulose fibrils are tightly connected to each other through hydrogen bonds. Microfibrillated cellulose can be prepared using a high-pressure homogenizer or Microfluidizer; however, most fibers obtained through only mechanical treatment are composed of CNF bundles rather than individual fibers. To obtain highly pure CNFs (highly homogeneous and containing only low amounts of microfibers), the fibrous suspensions should be subjected to mechanical treatment several times, an extremely energy-consuming process. CNF production can also be hindered by the clogging of the equipment, inevitably increasing production

[a]National Institute of Forest Science, 57 Hoegi-ro, Dongdaemun-gu, Seoul 02455, South Korea. E-mail: csj1730@korea.kr; gwonjg@korea.kr
[b]Daeshin University, 33 Gyeongcheong-ro 222-gil, Gyeongsan, Gyeongsangbukdo, 38649, South Korea
[c]Kookmin University, 77 Jeongneung-ro, Seongbuk-Gu, Seoul 02707, South Korea
[d]University of Seoul, 163 Seoulsiripdae-ro, Dongdaemun-gu, Seoul 02504, South Korea

† Electronic supplementary information (ESI) available. See DOI: https://doi.org/10.1039/d4ra04948a

costs. Hence, a chemical modification of cellulose is required before its mechanical treatment.

For improving CNF isolation, the formation of hydrogen bonds between cellulose fibers should be prevented by chemically substituting the hydroxyl group of the fibers before mechanical fibrillation. The oxidation of cellulose using the 2,2,6,6-tetramethylpiperidine-1-oxyl (TEMPO) radical as a functional catalyst is one of the most widely used modes of chemical modification. The regioselective oxidation of cellulose using the aminoxyl radical transforms the hydroxyl groups on the surface of cellulose into the negatively charged carboxyl group, which promotes nano-fibrillation.[13] The electrostatic repulsive force arising from the negatively charged surface can help generate individual nanofibers and maintain a stable colloidal dispersion. In other words, if the concentration of the carboxyl group is sufficiently high, even a mild mechanical treatment is adequate to partly convert cellulose into nano-sized materials.[14] The production of celluloses with many negatively charged groups could be a cost-effective approach for CNF production, as it reduces the energy consumption during nano-fibrillation.[15] As Isogai *et al.*[16] demonstrated the nano-sizing effect of the TEMPO oxidation system, many studies conducted on the system have established it as the most effective chemical pretreatment method to convert micro-sized cellulose fibers into nanoscale fibers. Furthermore, to comply with carbon reduction policies and promote environmentally sustainable technological advancements in the materials field, numerous CNF companies are directing their efforts to manufacture CNFs using the proven TEMPO system for high-value applications. However, end-product manufacturers hesitate to adopt the final applications of CNFs owing to the perceived high cost of the catalyst used in TEMPO oxidation, thus hindering the commercialization of CNFs despite their advantages.[17]

This issue must be addressed to realize CNF applications at the industrial level; hence, several studies have been recently conducted to reduce the final cost of CNF production.[18–20] A cost-effective method to manufacture CNF is to lower the cost of pretreatment, for instance, by optimizing the amounts of the reagents consumed. Xu *et al.*[21] reported that the amount of catalyst in a TEMPO-mediated system significantly affects the oxidant consumption rate, whereas excessive concentrations of TEMPO and NaBr increase the production cost unnecessarily with yields similar to those from the nano-fibrillation of cellulose. The reasons outlined above explain why research on improving the efficiency of the traditional TEMPO oxidation system has recently regained significant attention. Several studies focused on the cost-effective production of oxidized CNF within a given TEMPO system have centered on optimizing reaction conditions (such as the control of pH and time),[22–24] introducing a new TEMPO system (*e.g.*, traditional TEMPO system/$NaClO_2$ or/Na_2SO_4),[21,25–28] and developing new equipment for oxidation treatment capable of high-concentration pulp.[29] However, research aimed at reducing the high cost of the TEMPO catalyst has relatively received little attention.

Scheme 1 in the text illustrates the well-established reaction mechanism of a TEMPO/NaBr/NaClO oxidation system. TEMPO and NaBr serve as a main- and co-catalyst, respectively, while NaClO is consumed as an oxidant for the protonation of TEMPO.[30] An assumption derived from this mechanism is that the additional oxidant under given conditions can drive the oxidation reaction further even with a reduced amount of TEMPO catalyst. Thus, the strategy of reducing the TEMPO catalyst can be an intuitive approach to significantly decrease the treatment cost of the traditional TEMPO system.

Another insufficient point for research on TEMPO-oxidized CNF production is that a little information has been provided on CNFs prepared using only fixed mechanical treatment (*i.e.*, 4 passes of high-pressure homogenizer at 600 bar[21,30]). In this case, the types of CNF considered for application are inevitably restricted, which may lead to hasty decisions on the possibility of improving the performance of final products that use CNFs. Providing various types of CNF, manufactured according to the carboxyl group content and the number of mechanical treatments over a wide experimental range, allows researchers in the

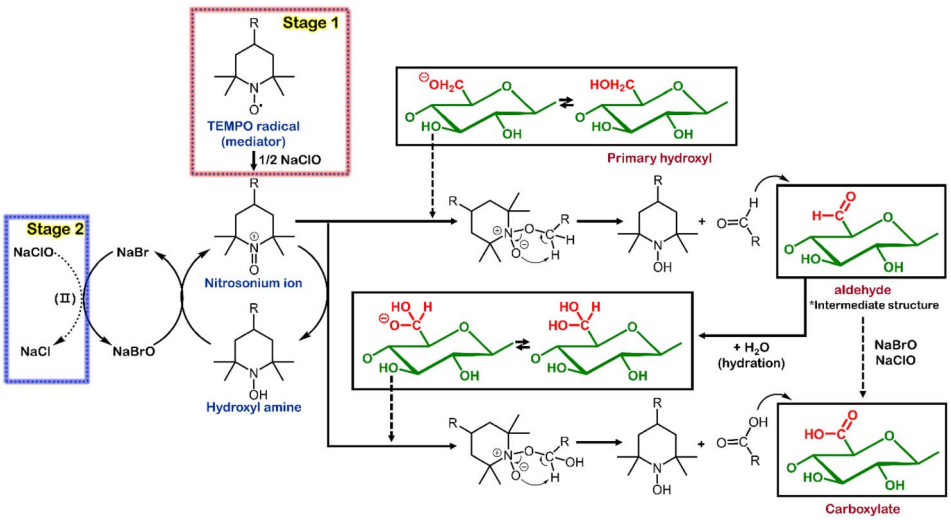

Scheme 1 Reaction mechanism of the TEMPO oxidation system (TEMPO/NaBr/NaClO).

field of advanced materials to make various strategies for improving the performance of the materials. Furthermore, if the advanced materials incorporating heterogenous CNF with low carboxyl content exhibit good performance, TEMPO-oxidized CNFs could be produced at an economical cost, which would be favorable for manufacturers of final products. Therefore, the attempts to offer various types of nanoparticles are crucial from an industrial angle. To our knowledge, no reports adopting this approach have yet been published.

Our current work primarily aims to oxidize hardwood-based pulp while reducing the usage of TEMPO (a costly catalyst) for controlling NaClO (a low-cost oxidant) and to provide various CNF forms by applying a wide experimental range of mechanical treatment. In particular, efforts were made to provide academic insights by analyzing changes in the chemical compositions, crystal structure, and the surface substitution degree of the cellulose based on the oxidation mechanisms. We tried to suggest guidelines for obtaining the optimal reagent consumption that can maximize the carboxylate content in micro-sized cellulose, and thoroughly examine the relationships between the carboxylate contents on the surface of micro-sized cellulose and the physiochemical properties (crystallinity, transmittance, dispersion stability, and morphologies) of the nanofibers prepared from the cellulose. Additionally, we hope to provide various options for types of TEMPO-oxidized CNFs to researchers or end-users in the field of advanced materials.

Experimental

Materials

A commercial hardwood bleached kraft pulp (MOORIM P&P CO., LTD Mixed H.W., Korea) was used for preparing TEMPO-oxidized CNFs (TOCNs). TEMPO (99%, Sigma-Aldrich, USA), sodium bromide (>99.5%, Junsei Chemical Co. Ltd, Japan), 12% sodium hypochlorite solution (12%, Yakuri Pure Chemicals Co., LTD, Japan), 0.5 N sodium hydroxide (0.5 N, Daejung Chemicals & Metals, Korea), and ethanol (99.5%, Daejung Chemicals & Metals, Korea) were used without further purification. Hydrogen chloride (0.1 N, Daejung Chemicals & Metals, Korea) and sodium chloride (Junsei Chemical Co. Ltd, 99.5%, Japan) were used to determine the content of the carboxylates. *tert*-Butanol (≥99.7%, Sigma-Aldrich, USA) was used as received for morphological analysis through the solvent-exchange process.

Preparation of TOCNs

To perform TEMPO oxidation, pulp sheets were torn into pieces approximately 3 × 3 cm in size. The pulp was then dried in an oven at 105 °C for 24 h to remove residual moisture. After drying, the pulp was cooled for 30 min at room temperature, and 20 g of the dried pulp were weighed and added to 1980 mL of distilled water. Subsequently, disintegration was carried out using a pulp disintegrator (L&W, Sweden) at 30 000 rpm. Pulp suspensions (1 wt%) containing TEMPO (0.05–0.5 mmol g^{-1}) and NaBr (1 mmol g^{-1}) were stirred at 400 rpm for 1 h at 25 °C. Subsequently, desired amounts of 12% NaClO (3–15 mmol g^{-1}) solution were added to initiate TEMPO-mediated oxidation. The pH was maintained at 10 by adding a 0.5 M NaOH solution for 2 h. Subsequently, 100 mL of ethanol was poured into the suspension to stop the oxidation. The suspension was then thoroughly washed with water *via* filtration. For preparing CNFs, the TEMPO-oxidized cellulose (TOC) was diluted to 0.5 wt%. To investigate the nano-fibrillation effects of TOC according to carboxylate content, TOCs with three types of carboxylated levels (0.65, 0.95, and 1.22 mmol g^{-1}) were chosen. The TOCs were homogenized at 150 MPa for 1–10 passes using a Microfluidizer (M-110EH-Microfluidizer®, Microfluidics, USA) consisting of two z-type chambers. The sizes of the chambers were 87 μm and 200 μm.

Chemical composition

Carbohydrates comprising a major portion of cellulose are polysaccharides primarily formed from glucose, xylose, arabinose, galactose, and mannose subunits. The concentrations of the polysaccharides can be determined by quantifying the sugar monomers obtained *via* sulfuric acid hydrolysis. The concentration of sugar in the TOCs and TOCNs was assessed *via* sulfuric acid hydrolysis following the protocol described in ASTM E1758-01. TOCs and TOCNs were oven-dried at 105 ± 1 °C for 24 h and stored in a desiccator. The dried sample was precisely weighed to 0.2 g and put into a vial containing 3 mL of 72% (w/w) sulfuric acid. The first acid hydrolysis was conducted for 2 h while stirring the mixture with a glass rod every 10 min. The hydrolyzed solution was subsequently poured into a serum bottle and diluted to the concentration of 4 wt% sulfuric acid by adding 115 mL of deionized water. The second acid hydrolysis was conducted at 121 °C for 1 h using an autoclave. The acid-hydrolyzed sample (1 mL) was filtered using a 0.45 μm membrane syringe filter (Whatman, GE Healthcare, UK) for quantifying the monosaccharides using high-pressure liquid chromatography (HPLC) (1290 Infinity II, Agilent Technologies, USA). An Aminex HPX-87H column (300 × 7.8 mm, Bio-Rad Laboratories, Inc., Hercules, CA, USA) and a refractive index detector (1290 Infinity LC, Agilent Technologies, Santa Clara, USA) were used for HPLC analysis. The column temperature was set to 40 °C, and 0.01 N sulfuric acid was used in the moving phase at a flow rate of 0.6 mL min^{-1}.

Determination of carboxylate content

The C6 primary hydroxyls of cellulose are selectively oxidized to the C6 carboxylate group by the TEMPO/NaBr/NaClO oxidation system at a pH between 10 and 11. The content of the carboxylate group in TOC was determined *via* the conductometric titration method. First, 0.01 M NaCl (5 mL) was added to 50 mL of the TOC diluted to 0.5 wt% and stirred adequately to prepare a well-dispersed suspension. HCl solution (0.1 M) was then added to adjust the pH to 2.5, as measured by a pH meter (Mettler Toledo, SevenCompact S210, USA). Adding 0.01 M NaOH solution to the above suspension initiated the titration. The NaOH solution was added at a rate of 1 mL min^{-1} until the pH of the suspension reached 10.5. The content of the TOC carboxylate was determined from the conductivity curves (Fig. S1†), and the changes in conductivity were recorded using

a portable conductometer (Metteler Toledo, Seven2Go S3, USA). Conductivity curves exhibit two discontinuities assigned to the presence of a strong acid (HCl) and a weak acid (–COOH). At the beginning of the reaction, the conductivity of the suspension decreases gradually owing to the neutralization of the HCl by NaOH. After the reaction with the entire volume of HCl (V_1, mL), the modified carboxylate group (–COOH) is neutralized. During this period, the conductivity curves exhibit a slow progression. At the end of the neutralization (V_2, mL), the conductivity of the suspension increases linearly again owing to NaOH accumulation. The carboxyl concentration was calculated using the following equation (eqn (1)).

$$\text{Carboxylate content } \left(\text{mmol } g_{\text{cellulose}}^{-1}\right) = \frac{((V_1 - V_2) \times M_{\text{NaOH}})}{W} \quad (1)$$

where M_{NaOH} is the molarity of the NaOH solution and W is the weight of cellulose.

Morphological properties

TOC and TOCN suspensions were diluted to 0.002 wt% (50 mL) and dispersed using an ultrasonicator (VCX130PB, Sonics & Materials Inc., USA) for 90 s. Subsequently, the suspensions were vacuum-filtrated using a polytetrafluoroethylene (PTFE) membrane filter with a pore size of 0.2 μm (ADVANTEC®, Toyo Roshi Kaisha Ltd, Japan). The filtrated TOC and TOCN suspensions were immersed in *tert*-butanol three times (30, 30, and 90 min) to completely substitute water with the *tert*-butanol. The solvent-exchanged celluloses were stored in a deep freezer (DF8020S, Ilshinbiobase, Korea) at −60 °C for 24 h and then lyophilized in a freeze-dryer (LP-03, Ilshinbiobase, Korea) for 3 days to evaporate the *tert*-butanol. The freeze-dried samples were coated with iridium using a high-vacuum sputter coater (EMACE600, Leica Microsystems, Ltd, Germany). The morphologies of the coated cellulose fibers were observed using a scanning electron microscope (SEM, S-4800, Hitachi, Ltd, Japan) at an accelerating voltage of 1–5 kV and a working distance of 8.9–9.2 mm. From the SEM images (Fig. S2 and S3†), 50 and 300 measurements were randomly chosen for TOCs and TOCNs, respectively, using the Image J software to calculate the average diameter of the fibers.

Crystal and chemical structures

For examining the crystal structure, 0.5 wt% of the TOC suspensions were vacuum-filtrated and then oven-dried at 105 ± 1 °C. The crystal structure of the dried samples was observed using an X-ray diffractometer (DMAX-2500, Rigaku, Japan) with monochromatic Cu Kα radiation at 40 kV and 200 mA. The scan speed was set to 2° min^{-1}. The functional groups of the dried samples were observed using an attenuated total reflectance Fourier-transform infrared spectroscopy (ATR-FTIR, NiCOLET-iS10, Thermo Scientific, United States) with a wavenumber range of 600 to 4000 cm^{-1} performing 32 scans. Fig. S4† shows the FTIR spectra as a function of carboxyl group content. For the three carboxyl group contents (0.65, 0.95, and 1.22 mmol g^{-1}), an intensive peak around 1600 cm^{-1} corresponding to the C=O stretching bond was observed, confirming the presence of carboxylate groups as a result of the TEMPO oxidation treatment.[31–33] In contrast, the non-oxidized pulp (pristine) showed a peak around 1635 cm^{-1} corresponding to the –OH bending vibrations of cellulose, indicating the changes in functional groups resulting from the TEMPO oxidation treatment. The peaks around 2930–2850 cm^{-1} correspond to the asymmetric and symmetric stretching vibrations of the C–H groups, while the broad absorption band around 3450–3200 cm^{-1} corresponds to O–H stretching vibrations due to hydrogen bonding.[33] For the three carboxyl group contents, some C–H and –OH groups of cellulose can be converted to carboxyl groups due to TEMPO-oxidation treatment, which results in peaks with reduced intensity around 2930–2850 cm^{-1} and 3450–3200 cm^{-1} regions.

Colloidal properties

The surface charge of the obtained TOCNs was analyzed using a zeta potential analyzer (Zetasizer Nano ZSP, Malvern Panalytical Ltd, UK) at 25 °C. The concentration of TOCN suspensions was 0.1 wt%, with the zeta potential of each sample calculated using Henry's equation (eqn (2)). The average value was obtained from three repeated measurements.

$$U_{\text{E}} = \frac{2\varepsilon\zeta}{3\eta} f(\kappa\alpha), \quad (2)$$

where U_{E} is the electrophoretic mobility (μm cm V^{-1} s^{-1}), ε is the dielectric constant, ζ is the zeta potential (mV), η is the viscosity (cP), and $f(\kappa\alpha)$ is Henry's function.[34] For analyzing the light transmittance from the TOCN dispersions, all samples were diluted to a solid concentration of 0.5 wt% and analyzed using a UV-visible spectrophotometer (OPTIZEN POP, K-LAB Co., Ltd, Korea) in the wavelength range of 800–200 nm.

Results and discussion

Optimization of TOC reagent consumption

The TEMPO-mediated oxidation was optimized as a pretreatment for manufacturing high-quality, homogenous CNFs through mechanical processes. Fig. 1 and 2 show the physicochemical properties of the TOCs prepared using the TEMPO/NaBr/NaClO oxidation system with controlled amounts of TEMPO (0.05–0.5 mmol g^{-1}) and NaClO (3–15 mmol g^{-1}). Fig. 1a shows the amount of sugar in each monomer constituting the TOCs for various TEMPO concentrations. The bleached kraft pulp used in this study is composed of two major components: cellulose, a linear polymer composed of hexose sugar (glucose), and hemicellulose, a complex branched polymer composed of pentose sugar (xylose and other sugar derivatives). The TEMPO/NaBr/NaClO oxidation reduced the amounts of both glucose and xylose, implying that TEMPO-mediated oxidation can affect cellulose and hemicellulose hydrolysis. Consequently, the total concentration of sugar in the TOCs was reduced by approximately 29–32%, and the amount of sugar reduced slightly decreased with increasing TEMPO concentration (Fig. S5a†); otherwise, the XRD peaks of TEMPO-

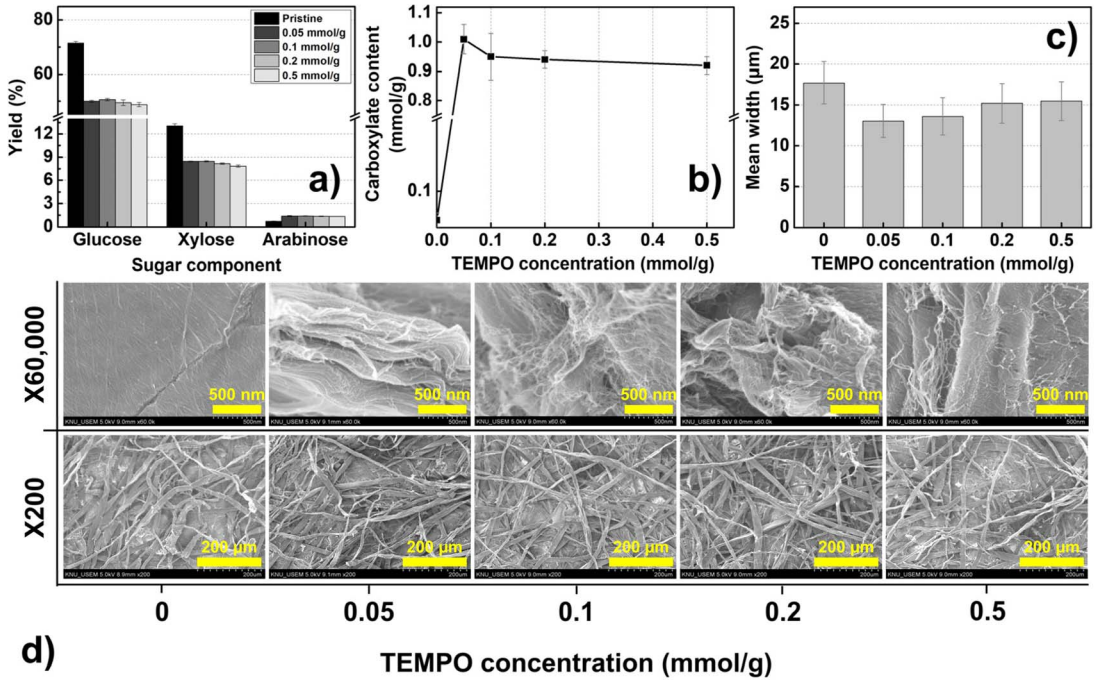

Fig. 1 Properties of TOCs for various concentrations of TEMPO: (a) yield of sugar components, (b) carboxylate content, (c) mean width, and (d) surface images of TOCs.

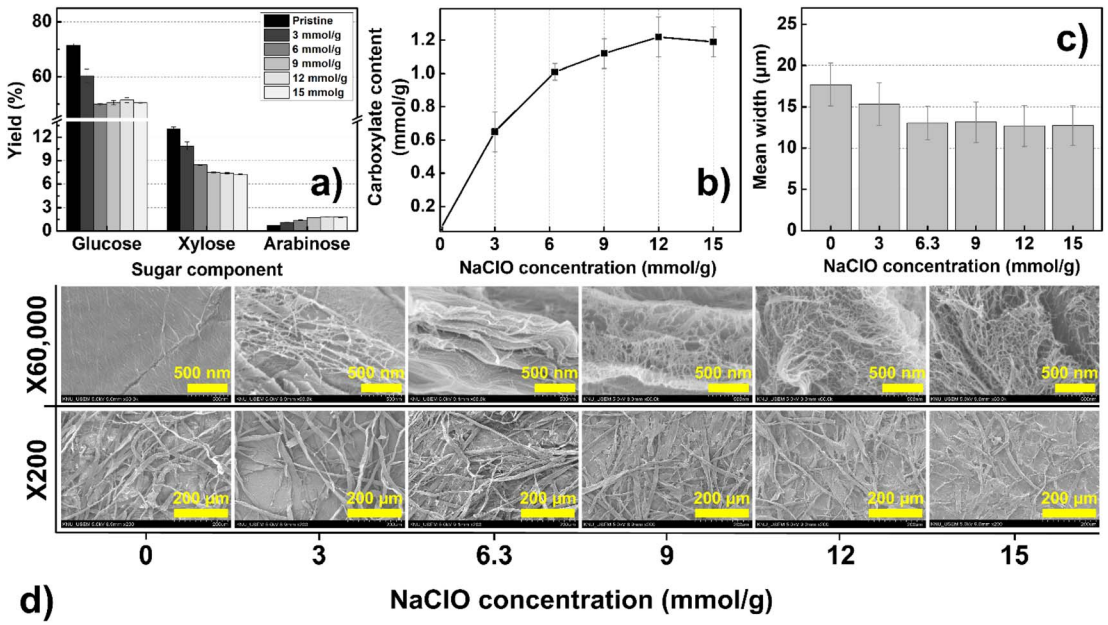

Fig. 2 Properties of TOCs for various concentrations of NaClO: (a) yield of sugar components, (b) carboxylate content, (c) mean width, and (d) surface images of TOCs.

oxidized cellulose were observed at approximately $2\theta = 15°$ (1–10), 16.3° (110), and 22.5° (200). These peak patterns are characteristic of natural cellulose (cellulose Iβ), indicating that the crystalline structure of cellulose remains unchanged during the TEMPO oxidation process. In contrast, when cellulose undergoes strong alkali treatment, dissolution, or regeneration, characteristic peak patterns appear at approximately $2\theta = 12°$ (1–10), 20° (110), and 22.6° (020). This transformation is indicative of a change to the cellulose II crystalline structure, which is influenced by alterations in the crystalline structure and hydrogen bonding of cellulose. The results suggest that the NaOH addition in the TEMPO oxidation reaction does not significantly affect the crystalline structure of cellulose and primarily acts on the amorphous regions[35,36] (Fig. S5b†). Fig. 1b

shows the concentration of carboxyl groups introduced onto the surface of the TOCs. When the amount of TEMPO added is 0.05 mmol g^{-1}, the content of the carboxylate groups increases remarkably from 0.06 to 1.01 mmol g^{-1} and then decreases slightly. A similar trend is observed even when a larger amount of TEMPO is added.

Notably, the carboxylate content increases despite a low TEMPO concentration within the designated reaction time. Initially, we assumed that a lower TEMPO concentration would lead to a slower oxidation reaction, resulting in fewer substituted carboxylate groups. However, as evident from Fig. 1b, the carboxylate content increases by 6.3% even when the amount of TEMPO is reduced from 0.1 mmol g^{-1} to 0.05 mmol g^{-1}, attributed to the limited quantity of the oxidant NaClO. Based on the literature,[16,37,38] we have outlined a simplified representation of the reactions within the TEMPO/NaBr/NaClO oxidation system in Scheme 1. NaClO is initially employed to activate the TEMPO catalyst (TEMPO → nitrosonium ion, stage I). Subsequently, NaClO is used to generate NaBrO for reactivating the hydroxylamine produced after the reaction of the nitrosonium ion (hydroxylamine → nitrosonium ion, stage II). A previous study[39] conducted on the reaction kinetics of TEMPO-mediated oxidation has reported that increasing the concentration of TEMPO increases the reaction rate (k_1), suggesting that NaClO is rapidly consumed to convert the TEMPO into the nitrosonium ion. Consequently, the amount of NaClO required to regenerate hydroxylamine, which is essential for activating NaBrO, decreases. Hence, an excess of TEMPO radical in the oxidation system could result in a low oxidation level of the C6 groups on the cellulose chain due to the lack of NaClO needed to reactivate the hydroxylamine–TEMPO. Another assumption is that, due to the limited amount of NaClO, it is difficult to deeply penetrate into the interior of micro-sized cellulose, resulting in a limited degree of substitution. The TEMPO oxidation mechanism rapidly consumes NaClO in the initial stages, substituting the C6 carbon on the surface of the cellulose particles. If penetration into the interior of the cellulose is difficult, the substitution reaction slows down, and the 1,4-β glycosidic bonds of the cellulose chains are attacked, breaking them down into amorphous short chains,[21] as evident from the decrease in the concentration of glucose shown in Fig. 1.

Further, as shown in Fig. 2a, an increase in NaClO concentration leads to a significant reduction in xylose, a sugar component of hemicellulose. The reduction in hemicellulose exposes a greater number of hydroxyl groups on the interior surface of the cellulose,[40] suggesting that deeper penetration in the cellulose particles may be possible[16] (Scheme 2). Therefore,

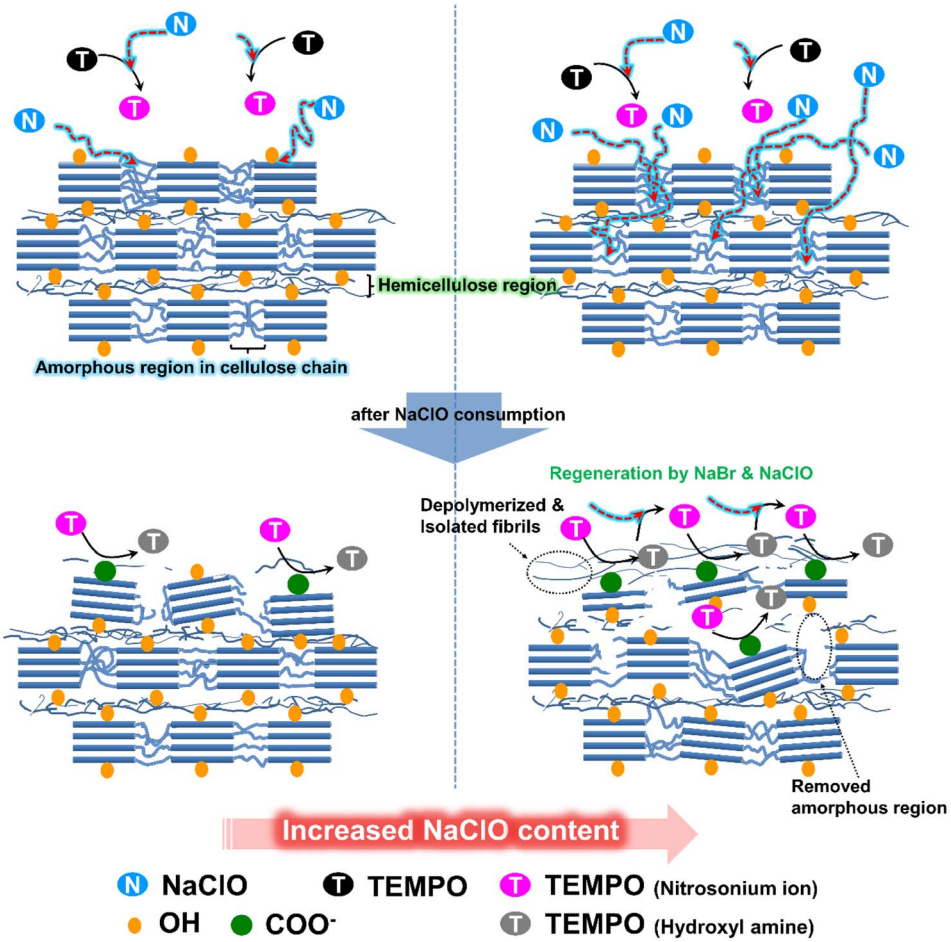

Scheme 2 Oxidation model on a cellulose surface when the concentration of NaClO is increased in the TEMPO system.

simply increasing the concentration of TEMPO with limited NaClO and reaction time may have restricted effects on increasing the quantity of the carboxyl group on the surface of cellulose particles. To some extent, these assumptions are supported by morphological analysis. Fig. 1c shows the mean width of TOCs as a function of the concentration of TEMPO. The mean width of cellulose fibers is the smallest at the TEMPO concentration corresponding to the highest content of carboxylates. The SEM images of the TOCs (Fig. 1d) reveal that the flat and clean surface of cellulose particles becomes rough after TEMPO oxidation, with pronounced wrinkling, particularly at the aforementioned TEMPO concentration.

An economically significant observation from Fig. 1 is that the amount of TEMPO consumed can be reduced to 0.05 mmol g^{-1} (the previously proposed protocol required 0.1 mmol g^{-1} of TEMPO)[41] while maintaining a high degree of fibrillation. Accordingly, the optimum amount of added TEMPO was determined as 0.05 mmol g^{-1}. Based on the oxidation reaction mechanism outlined in Scheme 1, we concluded that the surface substitution-related oxidation activity can be enhanced by increasing the amount of NaClO while keeping the TEMPO concentration constant. To prove this hypothesis, additional TEMPO-mediated oxidation was conducted by adjusting the concentration of NaClO, which is cheaper than TEMPO. NaClO was added at a concentration of 3–15 mmol g^{-1} to additionally increase the content of the carboxylate group and find an optimal point (at which maximum carboxylate content would be shown) for reagent consumption. Fig. 2a shows the sugar components in each monomer constituting the TOCs for various NaClO concentrations.

As explained in Schemes 1 and 2, hemicellulose and the amorphous regions of cellulose (xylose and glucose, respectively) decrease. The change in the amount of added NaClO alone decreases the total sugar content of the TOCs by approximately 15–30%; however, the reduction becomes insignificant after the concentration of NaClO exceeds 6.3 mmol g^{-1} (Fig. S5c†). Similar to Fig. S5b,† even with an increase in the amount of oxidant NaClO, the TEMPO-oxidized cellulose exhibited characteristic crystalline structure peaks at approximately $2\theta = 15°$ (1–10), 16.3° (110), and 22.5° (200). This indicates that the crystalline structure of cellulose remains unchanged during the TEMPO oxidation process (Fig. S5d†). Fig. 2b shows the content of carboxylates in the TOCs as a function of NaClO concentration. The maximum content of carboxylates (1.22 mmol g^{-1}) is obtained at 12 mmol g^{-1} of NaClO. The carboxylate content stabilizes at NaClO concentrations above 1.2 mmol g^{-1}. Fig. 2a and b clearly show that increasing the amount of NaClO can improve the activity of the catalysts (TEMPO and NaBrO) and their ability to reduce hemicellulose, which increases the content of the carboxylates without requiring additional TEMPO. The mean widths of the microfibers in the TOCs decreased from 17.7 to 12.2 μm, thus implying that the mean width was inversely proportional to the content of the carboxylate group (Fig. 2c). Distinct nano-sized web-like covers and several cracks were observed on the surface of the fibers (Fig. 2d); this tendency (especially nano-sized web-like covers) became more pronounced as the concentration of NaClO increased (Fig. S6†), indicating that nanofibers were produced despite the mild mechanical conditions (stirring at 400 rpm). These findings concerning the morphological characteristics of the TOCs support the hypothesis that the influence of NaClO can facilitate oxidation penetration to considerable depths, as explained above.

Effect of carboxylate content on the production of TOCNs

TOCs with three carboxylate contents (0.65, 0.95, and 1.22 mmol g^{-1}) were selected to examine the influence of the carboxylate content on pulp nano-fibrillation. The TOC suspensions were nano-fibrillated over 1, 5, and 10 passes using a Microfluidizer, and the physicochemical properties of the

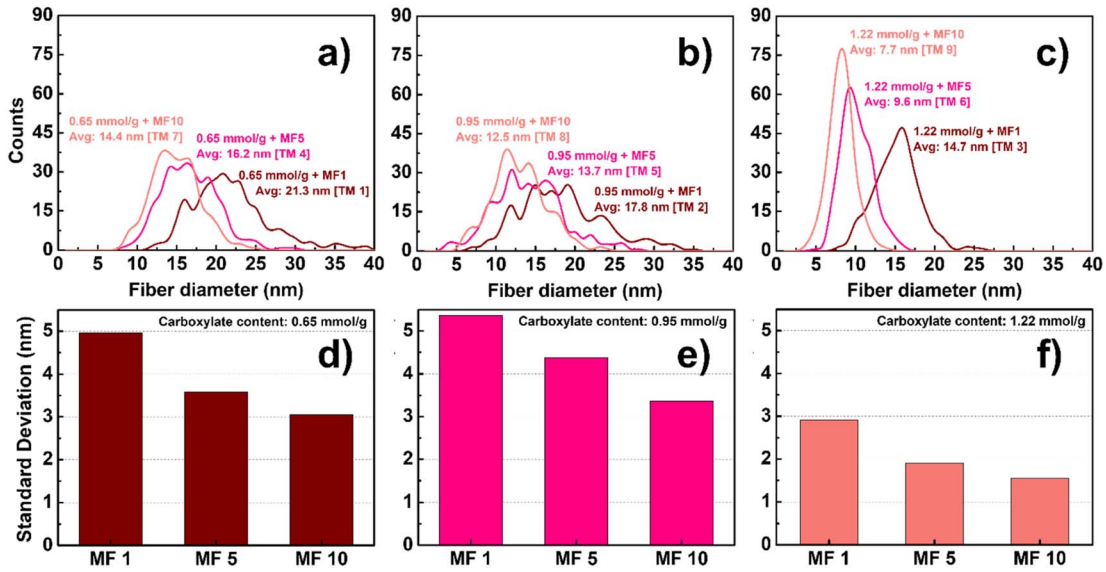

Fig. 3 Width distribution and its standard deviation for TOCNs with different carboxylate contents ((a and d) 0.65, (b and e) 0.95, and (c and f) 1.22 mmol g^{-1}).

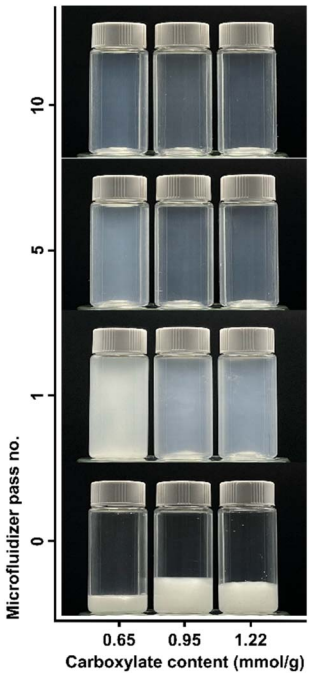

Fig. 4 Changes in the dispersion state of 0.5 wt% TOCs and TOCNs in water for different carboxylate contents and disintegration frequencies.

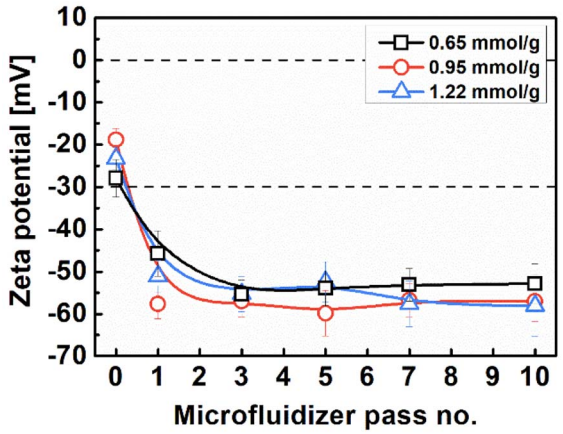

Fig. 5 Zeta potential of 0.1 wt% TOC and TOCN suspensions for different carboxylate contents and disintegration frequencies.

prepared suspensions and particles were analyzed. Fig. 3 shows the width distribution and standard deviation of individual cellulose nanoparticles for the three carboxylate contents. As expected, an increase in carboxylate content generally corresponds to a decrease in the thickness of the nanoparticles and an enhancement in uniformity. Furthermore, in the proposed optimized TEMPO oxidation system, the formation of predominantly individual nanofibers with nearly uniform sizes of approximately 7 nm was observed under the highest carboxylate content of 1.22 mmol g^{-1}.

Fig. 4 illustrates the dispersion stability and transparency of the 0.5 wt% colloidal suspension obtained. The transparency of the suspension increases with an increase in the carboxylate content and the number of Microfluidizer treatments. After processing the oxidized pulp using a Microfluidizer, variations in transparency were observed; however, the suspension remained stably dispersed even after a single treatment. We evaluated the zeta potential to precisely analyze this phenomenon, with the results presented in Fig. 5. Typically, colloidal suspensions with zeta potentials greater than ±30 mV are considered highly stable.[34,42] Colloidal suspensions with zeta potentials between ±10 and 30 mV exhibit initial instability, whereas those with zeta potentials between 0 and ±5 mV tend to coagulate rapidly. TEMPO oxidation treatment introduces a negative charge on the surface of cellulose particles. As the number of nano-sized particles increases owing to mechanical processing, the electrostatic repulsion from the surface negative charge can hinder particle aggregation. As evident from the zeta potential results, all TOCNs exhibited stable colloidal states with a high degree of dispersion, regardless of the carboxylate content. Therefore, the dispersion stability results showcase the effectiveness of the TEMPO oxidation treatment in producing highly dispersed TOCN suspensions. Fig. 6 shows the UV-vis transmittance results obtained for the 0.5 wt% TOCN suspensions prepared under different conditions. Each prepared TOCN was assigned a specific code based on its transmittance value (Table 1). Fig. 6a presents the behavior of data in the UV-visible range. For a more detailed analysis, the transmittance values at 500 nm are presented in Fig. 6b. In general, the transmittance increases as the carboxylate content and the number of mechanical treatments increase, with the highest transmittance obtained when the carboxylate content and the

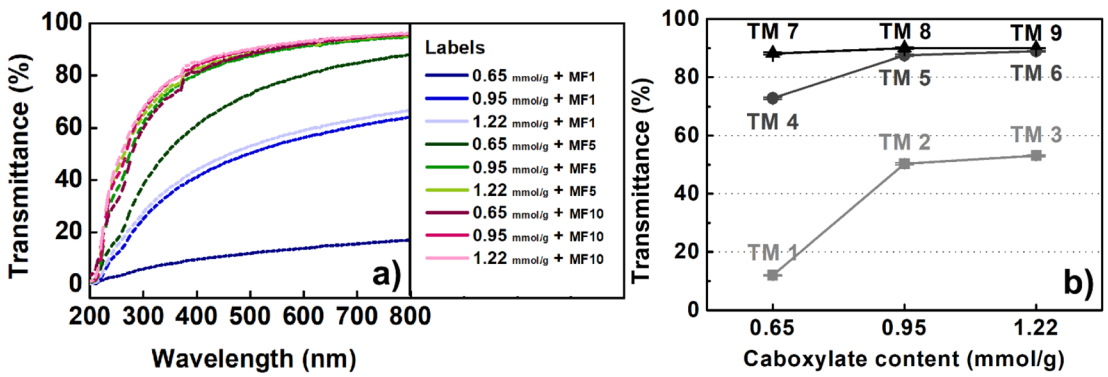

Fig. 6 UV-vis transmittance of TOCN suspensions (a) over a wide wavelength range and (b) at a wavelength of 500 nm.

Table 1 Sample codes of major TOCNs produced in this study

Microfluidizer pass no.	Carboxylate content (mmol g^{-1})		
	0.65	0.95	1.22
1	TM 1	TM 2	TM 3
5	TM 4	TM 5	TM 6
10	TM 7	TM 8	TM 9

number of treatments are 0.95 mmol g^{-1} and 5, respectively; similar values are maintained thereafter. Typically, the transmittance of a suspension varies depending on the size of particles, with the larger particles scattering more light and resulting in decreased transmittance.[41,43] However, notably, our UV-vis transmittance results were not well matched with the general trend. For instance, as observed in Fig. 3, the mean width of the nanoparticles obtained from celluloses with the carboxylate contents of 0.65 mmol g^{-1} and 1.22 mmol g^{-1} are 14.4 nm and 7.7 nm, respectively, after 10 Microfluidizer passes. The higher carboxylate content resulted in approximately 50% reduction in nanofiber size and a 50% increase in uniformity (standard deviation reduced from 3.1 to 1.6). By contrast, the increases in transmittance were approximately 88.1% and 89.9%, respectively, indicating similar values. Another notable observation is the significant differences in transmittance between conditions with similar average fiber thickness. As shown in Fig. 3, a comparison between the TM 2 and TM 3 conditions with the TM 4 and TM 7 conditions, respectively, reveals that the TM 4 and TM 7 conditions induce relatively high transmittance values, despite having similar nanofiber thickness (Fig. 6b).

To understand this phenomenon, we examined low-magnification images of the prepared suspensions, as shown in Fig. 7. Only nanoparticles were anticipated to be present in the suspensions under our experimental conditions. However,

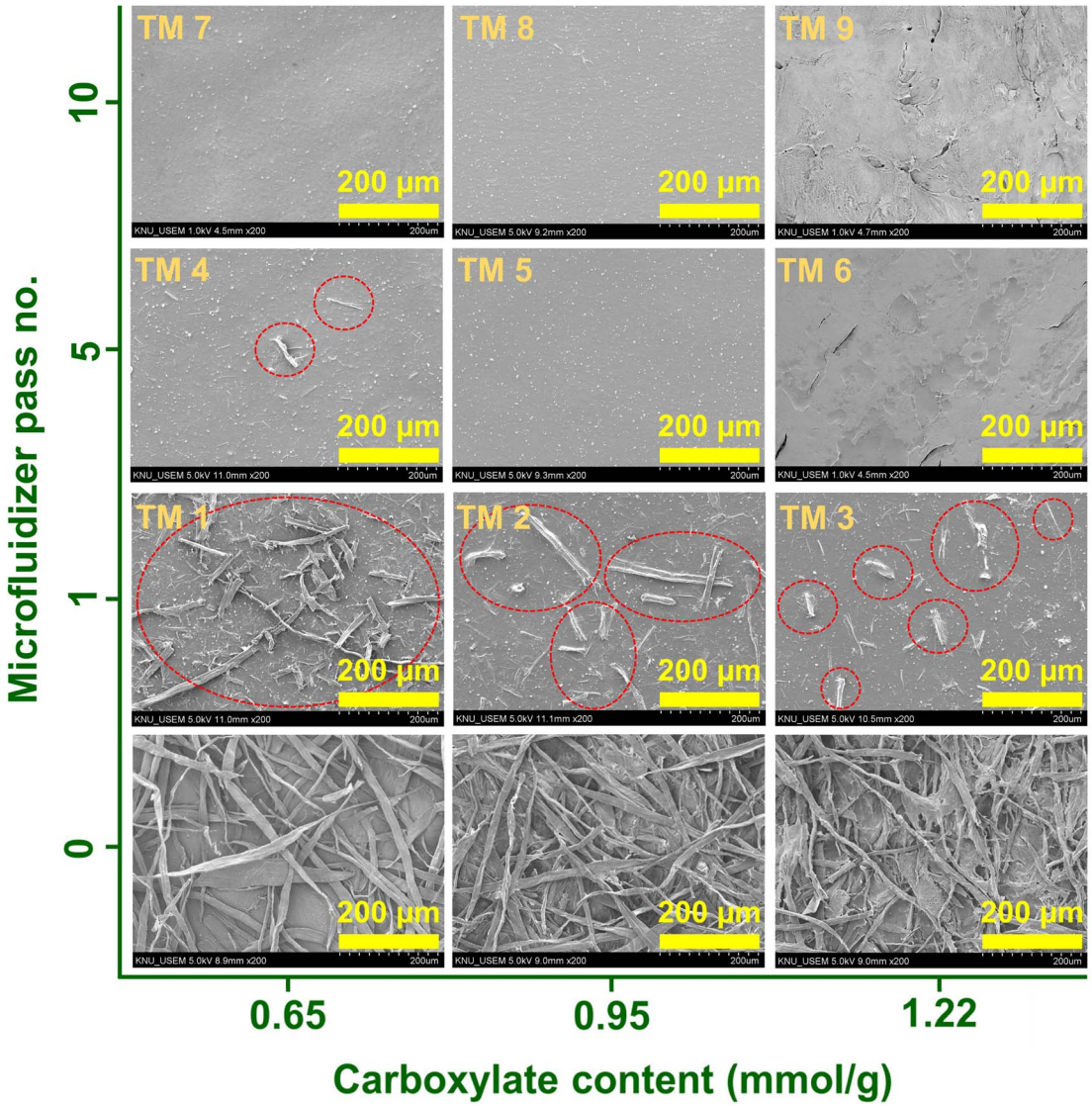

Fig. 7 SEM images of the particles in mechanical and/or TEMPO-oxidized TOCN suspensions.

we observed micro-sized fibers under conditions TM 1–TM 4. Furthermore, as carboxylate content and the number of mechanical treatments increased, the size and quantity of the micro-sized fibers (number of fibers within the circles in Fig. 7) tended to decrease. The trend exhibited by the presence and quantity of micro-sized fibers (Fig. 7) closely aligns with the trends exhibited by the UV-vis transmittance results (Fig. 6). Therefore, the presence of micro-sized fibers has a significant influence on UV transmittance, which is even greater than the influence of the nanoparticle size.[44] Our previous study conducted on the application of CNMs in polymer composites revealed that the agglomerates induced from nanoparticles act as defects, significantly reducing the mechanical properties of composites. Therefore, our interpretation of the UV-vis transmittance results is anticipated to provide meaningful insights for realizing applications requiring high-purity and highly dispersed CNMs, such as displays and polymer films.

Conclusions

In this work, a cost-effective TEMPO oxidation protocol was devised compared to the traditional TEMPO/NaBr/NaClO oxidation system. The hypothesis that NaClO oxidant plays a crucial role in increasing the reduced activity of the TEMPO catalyst even at a decreased catalyst dose has been proved. The optimal concentrations (having a maximum carboxylate content of 1.22 mmol g^{-1}) of TEMPO and NaClO were obtained as 0.05 mmol g^{-1} (a 50% reduction compared to the previous protocol) and 12 mmol g^{-1}, respectively. Nano-fibrillation of the cellulose treated by the improved TEMPO oxidation protocol was performed by the mechanical treatment using a Microfluidizer to explore a correlation between the carboxylate content and the production of the oxidized CNF. The nanoparticles formed within the fabricated CNF suspension exhibited a reduction in size and an increase in uniformity as the frequency of mechanical processing and the degree of cellulose surface substitution were elevated. Moreover, studies evaluating the suspension's characteristics using dispersion stability, UV-vis spectroscopy, and SEM imaging have suggested that a high-purity CNF suspension, free of microfibers, can be produced with a carboxylate content of 0.95 mmol g^{-1} or higher after more than five cycles of mechanical processing. Specifically, the interpretation of the relationship between UV and morphological images considered to assess the characteristics of the prepared oxidized CNF suspension suggests that UV is a promising approach for the rapid analysis of the purity of these suspensions. Our findings offer a practical way to control the quality of nano-dispersions obtained from the TEMPO oxidation system and suggest a feasible method to selectively provide CNMs according to the requirements of various applications.

Data availability

The data supporting this article have been included as part of the ESI.†

Author contributions

Jisoo Park: conceptualization, methodology, writing – original draft. Danbee Lee: methodology, investigation. Kyojung Hwang: methodology, formal analysis. Jimin Lee: methodology, validation. Tai-Ju Lee: writing – review & editing. Youngsu Kim: methodology, investigation. Jung Hyeun Kim: writing – review & editing. Jieun Lee: investigation. Won-Jae Youe: methodology, validation. Sang-Jin Chun: investigation, methodology, validation, writing – review & editing. Jaegyoung Gwon: conceptualization, methodology, writing – review & editing, supervision.

Conflicts of interest

There are no conflicts to declare.

Acknowledgements

This study was supported by the National Institute of Forest Science (grant number: FP0701-2021-02) and Korea Forest Service (grant number: 2021354A00-2023-AC03-1).

Notes and references

1 S. Liu, Z. X. Low, Z. Xie and H. Wang, *Adv. Mater. Technol.*, 2021, **6**, 2001180.
2 S. Chanda and D. S. Bajwa, *Rev. Adv. Mater. Sci.*, 2021, **60**, 325–341.
3 K. Abe, S. Iwamoto and H. Yano, *Biomacromolecules*, 2007, **8**, 3276–3278.
4 S. Iwamoto, A. N. Nakagaito and H. Yano, *Appl. Phys. A: Mater. Sci. Process.*, 2007, **89**, 461–466.
5 K. C. Cheng, C. F. Huang, Y. Wei and S. H. Hsu, *NPG Asia Mater.*, 2019, **1**, 25.
6 D. G. Hepworth and D. M. Bruce, *Composites, Part A*, 2000, **31**, 283–285.
7 M. Jarvis, *Nature*, 2003, **426**, 611–612.
8 T. Abitbol, A. Rivkin, Y. Cao, Y. Nevo, E. Abraham, T. Ben-Shalom, S. Lapidot and O. Shoseyov, *Curr. Opin. Biotechnol.*, 2016, **39**, 76–88.
9 M. A. Hubbe, A. Ferrer, P. Tyagi, Y. Yin, C. Salas, L. Pal and O. J. Rojas, *BioResources*, 2017, **12**, 2143–2233.
10 K. Köse, M. Mavlan and J. P. Youngblood, *Cellulose*, 2020, **27**, 2967–2990.
11 J. S. Park, C. W. Park, S. Y. Han, E. A. Lee, A. W. Cindradewi, J. K. Kim, G. J. Kwon, Y. H. Seo, W. J. Yoo, J. Gwon and S. H. Lee, *Polymers*, 2021, **13**, 1709.
12 T. H. Tan, H. V. Lee, W. A. Y. Dabdawb and S. B. B. O. Abd Hamid, *Materials for Biomedical Engineering*, 2019, pp. 131–164.
13 A. Isogai, T. Hänninen, S. Fujisawa and T. Saito, *Prog. Polym. Sci.*, 2018, **86**, 122–148.
14 A. Isogai and L. Bergström, *Curr. Opin. Green Sustainable Chem.*, 2018, **12**, 15–21.
15 T. Lindstrom, A. Naderi and A. Wiberg, *J. Korea Tech. Assoc. Pulp Pap. Ind.*, 2015, **47**, 5–21.

16 A. Isogai, T. Saito and H. Fukuzumi, *Nanoscale*, 2011, **3**, 71–85.
17 S. R. Djafari Petroudy, B. Chabot, E. Loranger, M. Naebe, J. Shojaeiarani, S. Gharehkhani, B. Ahvazi, J. Hu and S. Thomas, *Energies*, 2021, **14**, 6792.
18 S. R. D. Petroudy, A. Ghasemian, H. Resalati, K. Syverud and G. Chinga-Carrasco, *Cellulose*, 2015, **22**, 385–395.
19 I. Solala, A. Volperts, A. Andersone, T. Dizhbite, N. Mironova-Ulmane, A. Vehniäinen, J. Pere and T. Vuorinen, *Holzforschung*, 2012, **66**, 477–483.
20 J. Pennells, I. D. Godwin, N. Amiralian and D. J. Martin, *Cellulose*, 2020, **27**, 575–593.
21 H. Xu, J. L. Sanchez-Salvador, A. Balea, A. Blanco and C. Negro, *Cellulose*, 2022, **29**, 6611–6627.
22 C. Lin, T. Zeng, Q. Wang, L. Huang, Y. Ni, F. Huang, X. Ma and S. Cao, *Bioresources*, 2018, **13**, 5965–5975.
23 T. Saito, Y. Nishiyama, J. L. Putaux, M. Vignon and A. Isogai, *Biomacromolecules*, 2006, **7**, 1687–1691.
24 T. T. T. Hop, D. T. Mai, T. D. Cong, T. T. Y. Nhi, V. D. Loi, N. T. M. Huong and N. T. Tung, *Results Chem.*, 2022, **4**, 100540.
25 T. Inamochi, R. Funahashi, Y. Nakamura, T. Saito and A. Isogai, *Cellulose*, 2017, **24**, 4097–4101.
26 M. Hirota, N. Tamura, T. Saito and A. Isogai, *Carbohydr. Polym.*, 2009, **78**, 330–335.
27 T. Saito, M. Hirota, N. Tamura, S. Kimura, H. Fukuzumi, L. Heux and A. Isogai, *Biomacromolecules*, 2009, **10**, 1992–1996.
28 T. Saito, M. Hirota, N. Tamura and A. Isogai, *J. Wood Sci.*, 2010, **56**, 227–232.
29 J. L. Sanchez-Salvador, H. Xu, A. Balea, A. Blanco and C. Negro, *Int. J. Biol. Macromol.*, 2024, **261**, 129612.
30 J. L. Sanchez-Salvador, C. Campano, C. Negro, M. C. Monte and A. Blanco, *Adv. Sustainable Syst.*, 2021, **5**, 2000277.
31 Z. Tang, X. Lin, M. Yu, A. K. Mondal and H. Wu, *Int. J. Biol. Macromol.*, 2023, **259**, 129081.
32 J. Levanic, M. Gericke, T. Heinze, I. Poljansek and P. Oven, *Cellulose*, 2020, **27**, 2053–2068.
33 S. Amine, A. Montembault, M. Fumagalli, A. Osorio-Madrazo and L. David, *Polymers*, 2021, **13**, 2023.
34 J. D. Clogston and A. K. Patri, *Methods Mol. Biol.*, 2011, **697**, 63–70.
35 M. E. Abd El-Aziz, S. M. M. Morsi, D. M. Salama, M. S. Elwahed, E. A. Shaaban and R. E. Abou-Zeid, *Carbohydr. Polym. Technol. Appl.*, 2023, **6**, 100388.
36 I. Carrillo-Varela, C. Vidal, S. Vidaurre, C. Parra, A. Machuca, R. Briones and R. T. Mendonca, *Polymers*, 2022, **14**, 3127.
37 W. F. Bailey, J. M. Bobbitt and K. B. Wiberg, *J. Org. Chem.*, 2007, **72**, 4504–4509.
38 S. Goldstein and A. Samuni, *J. Phys. Chem.*, 2007, **111**, 1066–1072.
39 A. Mazega, A. F. Santos, R. Aguado, Q. Tarrés, N. Fiol, M. À. Pèlach and M. Delgado-Aguilar, *Cellulose*, 2023, **30**, 1421–1436.
40 J. G. Gwon, S. Y. Lee, G. H. Doh and J. H. Kim, *J. Appl. Polym. Sci.*, 2010, **116**, 3212–3219.
41 T. Saito, S. Kimura, Y. Nishiyama and A. Isogai, *Biomacromolecules*, 2007, **8**, 2485–2491.
42 M. C. Li, Q. Wu, K. Song, S. Lee, Y. Qing and Y. Wu, *ACS Sustain. Chem. Eng.*, 2015, **3**, 821–832.
43 E. J. Foster, R. J. Moon, U. P. Agarwal, M. J. Bortner, J. Bras, S. Camarero-Espinosa, K. J. Chan, M. J. Clift, E. D. Cranston, S. J. Eichhorn and D. M. Fox, *Chem. Soc. Rev.*, 2018, **47**, 2609–2679.
44 J. J. Kaschuk, Y. A. Haj, J. V. Garcia, A. Kamppinen, O. J. Rojas, T. Abitbol, K. Miettunen and J. Vapaavuori, *Carbohydr. Polym.*, 2024, **332**, 121877.